

2022

## Towards fluoro-free interventions: Using radial intracardiac ultrasound for vascular navigation

Hareem Nisar  
*Western University, hnisar3@uwo.ca*

Leah Groves

Leandro Cardarelli-Leite

Terry M Peters  
*Imaging Research Laboratories, Robarts Research Institute, London, Ontario, Canada & Biomedical Engineering Graduate Program, Western University, London, Ontario, Canada & Department of Medical Biophysics, Western University, London, Ontario, Canada*

Elvis C.S. Chen  
*chene@robarts.ca*

Follow this and additional works at: <https://ir.lib.uwo.ca/robartspub>



Part of the [Bioimaging and Biomedical Optics Commons](#)

---

### Citation of this paper:

Nisar, Hareem; Groves, Leah; Cardarelli-Leite, Leandro; Peters, Terry M; and Chen, Elvis C.S., "Towards fluoro-free interventions: Using radial intracardiac ultrasound for vascular navigation" (2022). *Robarts Imaging Publications*. 26.

<https://ir.lib.uwo.ca/robartspub/26>

# Ultrasound in Medicine & Biology

## Towards fluoro-free interventions: Using radial intracardiac ultrasound for vascular navigation

--Manuscript Draft--

<b>Manuscript Number:</b>	
<b>Article Type:</b>	Original Contribution
<b>Keywords:</b>	Transcatheter interventions; Vascular navigation; Fluoro-free; Transfemoral guidance; Vascular Disease; Intracardiac echocardiography
<b>Corresponding Author:</b>	Hareem Nisar Western University London, ON CANADA
<b>First Author:</b>	Hareem Nisar
<b>Order of Authors:</b>	Hareem Nisar Leah Groves Leandro Cardarelli-Leite Terry M. Peters Elvis C.S. Chen
<b>Abstract:</b>	<p>Transcatheter cardio-vascular interventions have the advantage of patient safety, reduced surgery time, and minimal trauma to the patient's body. Transcatheter interventions, which are performed percutaneously, suffer from the lack of direct line-of-sight with the surgical tools and the patient anatomy. Therefore, such interventional procedures rely heavily on image guidance for navigating towards and delivering therapy at the target site. Vascular navigation via the inferior vena cava (IVC), from the groin to the heart, is an imperative part of most transcatheter cardiovascular interventions such as valve repair surgeries and ablation therapy. Traditionally, the IVC is navigated using fluoroscopic techniques such as angiography or CT venography. These X-ray based techniques can have detrimental effects on the patient as well as the surgical team, causing increased radiation exposure, increased risk of cancer, fetal defects, eye cataracts. The use of heavy lead apron has also been reported to cause back pain and spine issues thus leading to interventionalist's disc disease. We propose the use of a catheter-based ultrasound augmented with electromagnetic (EM) tracking technology to generate a vascular roadmap in real-time and perform navigation without harmful radiation. In this pilot study, we use intracardiac echocardiography (ICE) and tracking technology to reconstruct a vessel from a phantom in a 3D virtual space. This paper presents a pilot phantom study on ICE-based vessel reconstruction and demonstrates how the proposed ultrasound-based navigation will appear in a virtual space, by navigating a tracked guidewire within the vessels in the phantom without any radiation-based imaging. The geometric accuracy is assessed using a CT scan of the phantom, with a Dice coefficient of 0.79. The average distance between the surface of the two models comes out to be <math>1.7 \pm 1.12</math>mm.</p>
<b>Suggested Reviewers:</b>	
<b>Opposed Reviewers:</b>	

To,  
Christy K. Holland  
Editor-in-Chief,  
Ultrasound in Medicine and Biology (UMB)

Date: 20<sup>th</sup> August 2021

**Subject: Cover Letter for UMB submission – “Towards fluoro-free interventions: Using radial intracardiac ultrasound for vascular navigation”**

Dear Dr. Holland,

We are pleased to submit our research to the UMB journal. We state that this manuscript is of original contribution and has not and will not be submitted elsewhere for publication. The contribution from individual authors is stated as the following:

1. Hareem Nisar – primary researcher – design and execution of the study, performing all the experiments, most of the code generation, and writing the journal article.
2. Leah Groves – secondary researcher – part of the code generation, writing part of the paper, and editing the manuscript.
3. Leandro Cardarelli-Leite – clinical advisor – providing clinical motivation and regular insights towards the project, paper design, and editing.
4. Terry M. Peters – senior advisor – project supervision, grant holder, paper design and editing
5. Elvis C.S. Chen – senior advisor – project supervision, resource management, paper design, and editing.

All authors have individually approved the submission of this manuscript to UMB. Thank you for considering our submission.

In case of any query, please reach out to us at [hnisar3@uwo.ca](mailto:hnisar3@uwo.ca) or [chene@robarts.ca](mailto:chene@robarts.ca).

Best regards,

Hareem Nisar



# Towards fluoro-free interventions: Using radial intracardiac ultrasound for vascular navigation

Hareem Nisar<sup>a,b,\*</sup>, Leah Groves<sup>a,b</sup>, Leandro Cardarelli-Leite<sup>c</sup>, Terry M. Peters<sup>a,b,d</sup>, Elvis C.S. Chen<sup>a,b,d</sup>

<sup>a</sup>*Robarts Research Institute, Western University, London, ON, Canada*

<sup>b</sup>*Department of Biomedical Engineering, Western University, London, ON, Canada*

<sup>c</sup>*London Health Sciences Centre, London, ON, Canada*

<sup>d</sup>*Department of Medical Biophysics, Western University, London, ON, Canada*

---

## Abstract

Transcatheter cardio-vascular interventions have the advantage of patient safety, reduced surgery time, and minimal trauma to the patient's body. Transcatheter interventions, which are performed percutaneously are limited by the lack of direct line-of-sight with the surgical tools and the patient anatomy. Therefore, such interventional procedures rely heavily on image guidance for navigating towards and delivering therapy at the target site. Vascular navigation via the inferior vena cava (IVC), from the groin to the heart, is an imperative part of most transcatheter cardiovascular interventions including heart valve repair surgeries and ablation therapy. Traditionally, the IVC is navigated using fluoroscopic techniques such as angiography or CT venography. These X-ray based techniques can have detrimental effects on the patient as well as the surgical team, causing increased radiation exposure, leading to risk of cancer, fetal defects, and eye cataracts. The use

---

\*Corresponding Author: Hareem Nisar, Robarts Research Institute, 1151 Richmond St. N. London, ON N6A 5B7; Email, hnisar3@uwo.ca; Phone, 519.931.5777

of heavy lead apron has also been reported to cause back pain and spine issues thus leading to interventionalist's disc disease. We propose the use of a catheter-based ultrasound augmented with electromagnetic (EM) tracking technology to generate a vascular roadmap in real-time and perform navigation without harmful radiation. In this pilot study, we use spatially-tracked intracardiac echocardiography (ICE) to reconstruct a vessel from a phantom in a 3D virtual environment. We demonstrate how the proposed ultrasound-based navigation will appear in a virtual environment, by navigating a tracked guidewire within the vessels in the phantom without any radiation-based imaging. The geometric accuracy is assessed using a CT scan of the phantom, with a Dice coefficient of 0.79. The average distance between the surface of the two models comes out to be  $1.7 \pm 1.12$  mm.

*Keywords:* Transcatheter interventions, Vascular navigation, Fluoro-free, Transfemoral guidance, Vascular Disease

---

## 1 **Introduction**

2 Advances in medical imaging, combined with miniaturized and flexible  
3 surgical tools, have allowed surgical procedures to be performed percuta-  
4 neously using transcatheter-based approaches. These minimally invasive ap-  
5 proaches have increased patient safety, decreased procedure time, and low-  
6 ered complication rates (Jahangiri et al., 2019). Catheter-directed therapies  
7 inherently prohibits the direct line-of-sight with the anatomy and the tools.  
8 Interventionalists rely heavily on image-guidance to navigate and position  
9 their tools to deliver therapy at the target region. Common imaging modal-  
10 ities used for transcatheter-based interventions include X-ray fluoroscopy,  
11 computed tomography (CT), magnetic resonance imaging (MRI), and in-  
12 travascular (IVUS), intracardiac (ICE) or transesophageal (TEE) ultrasound  
13 (US).

14 Fluoroscopy is commonly used for minimally invasive procedures as it pro-  
15 vides real-time, high contrast vascular images, by means of X-ray imaging  
16 with contrast enhancement. The radiation exposure produced by X-rays can  
17 be harmful to the patient, clinical staff, and medical trainees, even when used  
18 in conjunction with various shielding techniques (Theocharopoulos et al.,  
19 2006; Christopoulos et al., 2016). The use of heavy shielding aprons may have  
20 detrimental effects on the physical health of the interventional team causing  
21 "interventionalist's disc disease" (Ross et al., 1997) which includes back and  
22 neck pain (Dixon et al., 2017), cervical disc herniation, and other spinal and  
23 musculoskeletal issues (Goldstein et al., 2004), as well as the possibility of  
24 lead poisoning (Katsari et al., 2020). Interventional cardiologists and radiol-  
25 ogists have reported developing eye cataracts (Jacob et al., 2013), increased

26 risk of cancer (Roguin et al., 2013), and increased risk of fetal congenital  
27 defects (Limacher et al., 1998). The use of contrast agents to compensate  
28 for the lack of soft-tissue visualization in X-rays can induce complications  
29 for patients with renal impairments and allergic reactions (Davenport et al.,  
30 2015).

31 Due to its high resolution and large field of view, pre-operative CT is  
32 a standard of care for vascular mapping and assessment of intravascular  
33 pathology (Murphy et al., 2018). However, CT imaging is typically used  
34 for diagnostic and pre-surgical planning, and is limited in its use for real-  
35 time surgical navigation. CT is also based on ionizing radiation and carries  
36 the same risks previously described for fluoroscopy. Furthermore, the surgery  
37 cannot be performed with the patient within the CT bore. In transcatheter  
38 procedures, there is an unmet need for safe, reliable, radiation-free and real-  
39 time image-guidance during vascular navigation.

40 In efforts of minimizing the radiation exposure in Cath labs, near-zero  
41 fluoro methods and no-fluoro surgical workflows have also been proposed in  
42 the literature (Stec et al., 2014; Zhang et al., 2020) to guide the catheters  
43 during an ablation procedure and perform transseptal puncture using ICE.  
44 Alternative imaging modalities such as MR, and US are also considered.  
45 Vascular navigation is fundamental to transcatheter cardiac interventions  
46 such as transcatheter aortic valve implantation (TAVI), caval-valve implan-  
47 tation, and mitral and tricuspid valve annuloplasty, repair and replacement  
48 surgeries (Prendergast et al., 2019). Accurate representation of the vessel  
49 geometry is not only important for navigation towards the target site, but  
50 also for delivering the optimal therapy (Murphy et al., 2017; Shammass et al.,

51 2019). Procedures such as angioplasty, stent placement, IVC filtration all  
52 rely on vascular imaging to locate the pathological vessel region, select an  
53 appropriately sized device, and deploy the balloon or stent correctly.

54 Catheter-based US technologies such as intravascular US (IVUS) and  
55 intracardiac echo (ICE) are already indispensable components of Cardiac  
56 Catheterization labs (Cath Lab), assisting in the assessment of the disease  
57 and device placement. The recent introduction of optical US (OpUS) tech-  
58 nology also shows the great potential for the use of catheter-based US for  
59 cardiovascular interventions (Little et al., 2020). US offers a radiation-free  
60 alternative for real-time image guidance. When combined with EM tracking  
61 technology, it offers the potential for a large-scale 3D US volume reconstruc-  
62 tion, visualization of anatomy, as well as real-time tool tracking. For most  
63 transcatheter interventions, there are two surgical phases - navigation of tools  
64 towards the target site and positioning of tools to deliver the treatment. In  
65 the case of cardiac interventions, vascular navigation is an imperative prereq-  
66 uisite. Either transfemoral, transradial or transjugular access is required to  
67 guide the catheters towards the heart. Inferior vena cava (IVC) navigation,  
68 from the groin to the chest, is one of the most common techniques in cardi-  
69 ology and is traditionally guided by fluoroscopy. In this paper, the targeted  
70 clinical application is the IVC navigation performed during transcatheter  
71 cardiovascular interventions.

72 We propose the use of tracked US as an alternative to CT-based vascular  
73 mapping and fluoro-guided tool navigation. Instead of using radiation-based  
74 imaging to navigate the tools, we propose the following surgical workflow:  
75 Prior to the intervention, a tracked, catheter-based US probe (such as ICE,

76 IVUS, or OpUS) scans the desired vasculature and a virtual 3D roadmap is  
77 reconstructed. This vascular path can then be easily traversed by a tracked  
78 tool or guidewire. This workflow eliminates radiation exposure and the use  
79 of heavy lead equipment. Such a system can also be used to make measure-  
80 ments of the vessel anatomy and intraluminal buildup. Ultrasound catheters  
81 including ICE and IVUS, as well as EM tracking technology are already an  
82 indispensable part of a Cath Lab and are used in electrophysiology proce-  
83 dures. The proposed ultrasound-based workflow has several advantages over  
84 the conventional fluoroscopic techniques. Apart from the lack of radiation,  
85 and heavy lead shielding equipment, an US-based navigation system offers  
86 full 3D visualization of anatomy, and provides more information to the clin-  
87 ician. Furthermore, the use of EM tracking technology allows for tracked  
88 tools and catheters which can result in an engaged and informative experi-  
89 ence for the clinicians. These features greatly reduce the cognitive load faced  
90 by the interventionalists and will potentially result in enhanced procedural  
91 outcome as well.

92 In this study, we utilized a Foresight ICE system – an intracardiac ul-  
93 trasound probe which involves a single-element transducer, spinning on its  
94 axis and tilted at a user-specified angle. As a result, the ultrasound image  
95 produced is a 2D conical surface image lying in 3D space. One of the biggest  
96 advantages of using this probe for navigation is the ‘Forward-viewing’ feature  
97 which allows the clinicians to watch where they are going as they traverse  
98 the vessels, thus improving their experience and adding a layer of procedural  
99 safety. The use of ICE probe is not limited to navigation. For transcatheter  
100 cardiac interventions, the ultrasound can further facilitate the delivery of

101 therapy or treatment. This study is geared towards the navigation of inferior  
102 vena cava (IVC), it also has the potential to be applied to the navigation  
103 of other vessels as well. IVC has many tributaries, but they need not to  
104 be navigated for cardiac procedures. The geometry of IVC is also compar-  
105 atively simpler than its tributaries like hepatic veins. Since the IVC passes  
106 through the entire length of the abdomen, it's surrounding tissues and organs  
107 vary along the length. Thus, the appearance of the IVC in the ultrasound  
108 varies as well. All these physical and echogenic attributes of IVC are diffi-  
109 cult to capture in one phantom. Therefore, for this first, phantom study we  
110 are demonstrating the concept on an ultrasound-realistic phantom represent-  
111 ing the infrarenal portion of the IVC. The goal is to reconstruct a vascular  
112 roadmap without any radiations, safely navigate the guidewire through the  
113 vessel, and visualize the guiding catheters as they ascend towards the heart.

114 This paper presents a pilot phantom study as a proof of concept to  
115 demonstrate the idea and feasibility of an US-based vascular navigation sys-  
116 tem for transcatheter interventions. A vascular phantom was scanned and  
117 reconstructed using a forward-looking radial ICE probe and EM tracking  
118 technology. The method details, open-source implementation, and phan-  
119 tom images are available online for reproducibility ([https://github.com/  
120 hareem-nisar/VascularNavigation](https://github.com/hareem-nisar/VascularNavigation)). The US-generated vessel model is  
121 validated against a CT-scan of the vessel phantom. For a visual validation  
122 and concept demonstration of real-time guidance, we also demonstrate nav-  
123 igation of a tracked guide-wire in a vascular phantom using the proposed  
124 US-based approach.

## 125 **Materials and Methods**

### 126 *Data Acquisition*

127 A polyvinyl alcohol cryogel (PVA-C) vascular phantom was manufactured  
128 to imitate the infra-renal portion of the IVC (Nisar et al., 2020). The phan-  
129 tom generated realistic US imaging when scanned by an intravascular (IVUS)  
130 or intracardiac (ICE) US, thus displaying a vessel-mimicking layer, blood-  
131 mimicking fluid in the lumen, and a surrounding tissue-mimicking layer. In  
132 this study, a 10 Fr, forward-looking, Foresight™(Conavi Medical Inc., North  
133 York, ON, Canada) ICE catheter was used to image the phantom. This  
134 probe generates 3D conical surface images, where the angle of the cone is  
135 user adjustable. The conical images are projected on a conventional monitor  
136 screen as viewed from the apex of the cone and displayed as a circular im-  
137 age. A digital frame-grabber (DVI2USB 3.0, Epiphan Video, Ottawa, ON,  
138 Canada) was used to capture the projected ICE images, and the cone-angle  
139 information from the console. For US tracking, the ICE probe was rigidly in-  
140 strumented with a 6DoF pose sensor (Aurora, NDI, Waterloo, ON, Canada)  
141 and spatially calibrated using a point-to-line Procrustean approach (Chen  
142 et al., 2016; Nisar et al., 2019).

143 The vessel phantom was placed in a large water-bath at room-temperature  
144 (Fig. 1). The main vessel of the phantom was scanned using the tracked  
145 ICE probe at an imaging depth of 80 mm, imaging angle of  $67^\circ$  and 12 MHz  
146 frequency. Due to some hardware constraints in our set-up, we were only  
147 able to scan the central vessel of the phantom and not the branches (details  
148 in Discussion section). US images were acquired in real-time using screen-  
149 capture. The imaging and tracking data were then processed to reconstruct

150 the surface representation of the vessel from the phantom. The data acqui-  
151 sition, vascular roadmap generation, and the user interface for navigation  
152 were all implemented as an open-source software using 3D Slicer (Fedorov  
153 et al., 2012). The steps involved in the automatic generation of the 3D  
154 vascular roadmap include pre-processing to remove image artifacts, lumen  
155 segmentation from 2D images and reconstruction of the vessel based on the  
156 segmentations and tracking information.

### 157 *Pre-processing*

158 The acquired screen-captures were cropped to remove any information  
159 outside of the US image. The bright reflections in the middle of the cropped  
160 US image represent an artifact inherent to the ICE probe (Fig. 2a). This  
161 artifact was minimized by using optimal display settings (third level 'wand'  
162 function) on the console, and later masking the central bright pixels in the  
163 image in our software. The time-gain compensation settings on the console  
164 were used to suppress the reflections from the phantom boundary and the  
165 container walls. A noise removing filter called the curve flow filter was applied  
166 to images to eliminate the interference from by the EM tracker (Fig. 2a) while  
167 preserving the contours of the vessel boundary. This was a necessary step  
168 prior to performing image processing for lumen segmentation.

### 169 *Lumen Segmentation*

170 Distinct from imaging using hand-held percutaneous US transducer, the  
171 shape of the vessel wall can vary significantly for catheter-based US. Since the  
172 US catheters travel through the vasculature adhering close to the vessel wall,  
173 the wall does not always appear as a closed circle in the case of radial IVUS

174 and ICE imaging. The first few millimeters of ICE imaging are corrupted by  
175 a ring artifact inherent to the radial ICE probe (Fig. 2a). As such, when the  
176 ICE catheter is clinging to the vessel wall, the reflection is interrupted close to  
177 the center of the image (Fig. 2a) and the vessel boundary appears C-shaped.  
178 Therefore, in this study, an edge-based approach was used to segment the  
179 vessel lumen from the ICE images, minimizing the error/leakages caused by  
180 a discontinuous vessel boundary. A statistics-based active contour algorithm  
181 was applied (Gao et al., 2010). This algorithm grows the boundaries of an  
182 initial seed based on the characteristics of the underlying image intensities,  
183 and can be manipulated by the parameters ‘intensity homogeneity’ (set to  
184 0.8) and ‘boundary smoothness’ (set to 1) to maintain the roundness of the  
185 contour and minimize leakages based on intensity.

186 The performance of the segmentation algorithm is highly dependent on  
187 the size and placement of the initial seed. Therefore, for the algorithm to  
188 be effective, it is necessary to have an initial seed, closely fitted to and com-  
189 pletely encapsulated and centered within the vessel lumen (Gao et al., 2010).  
190 The Hough transform was used to approximate the initial seed by fitting a  
191 circle to the lumen (Fig. 2b) (Parameters values: Hough Gradient,  $dp = 1$ ,  
192  $min\_dist = 100$ ,  $param1 = 95$ ,  $param2 = 20$ ). Gaussian blur was applied prior  
193 to the Hough transform to avoid over-detection of circles. To ensure that  
194 the seed does not overlap with the vessel boundary, the fitted circle was  
195 iteratively decreased in radius until there were no bright reflections in the  
196 underlying image. A hundred and eighty image frames were processed and  
197 2D lumen segmentations were acquired for each image.

198 *Vessel Reconstruction*

199 The Foresight™ICE probe generates forward-looking conical surface im-  
 200 ages. The images acquired by this device, and subsequently the lumen seg-  
 201 mentation, were a version of the true US data projected onto a 2D disk. 2D  
 202 lumen segmentations were subjected to 3D conversion to reconstruct true,  
 203 conical segmentations (Fig. 2c) using the radius and imaging angle informa-  
 204 tion, available through the console. This reconstruction is governed by the  
 205 equation:

$$\begin{bmatrix} x_{3D} \\ y_{3D} \\ z_{3D} \end{bmatrix} = \begin{bmatrix} 1 & 0 & -o_x \\ 0 & 1 & -o_y \\ 0 & 0 & \|(x_{2D}, y_{2D})\| \cdot \tan(90 - \phi) \end{bmatrix} \begin{bmatrix} x_{2D} \\ y_{2D} \\ 1 \end{bmatrix} \quad (1)$$

206 where  $(o_x, o_y)$  represents the center of the planar image or the apex of the  
 207 conical image, and  $\phi$  represents the imaging angle of the cone-shaped im-  
 208 age. Each segmentation was positioned and scaled to its correct shape and  
 209 location in 3D space by applying US probe calibration and tracking infor-  
 210 mation, producing a skeleton of the vessel (Fig. 3a). The vessel skeleton  
 211 was then processed to form a closed 3D surface representation using binary  
 212 morphological closing, with an annulus kernel of size  $[60, 60]$  to fill the gaps  
 213 between consecutive segments. For final smoothing of the reconstructed ves-  
 214 sel, a Gaussian blur with a standard deviation of 3 was applied. The result  
 215 represents the 3D model of the vessel scanned from our phantom (Fig. 3b),  
 216 spatially present in the EM tracker’s coordinate system.

217 *Validation*

218 As described previously, vascular navigation is currently achieved using  
219 fluoroscopy or CT mapping. The vessel phantom was imaged using US, and  
220 the vessel was reconstructed and compared with X-ray and CT. Geomet-  
221 ric accuracy of the US reconstructed vessel model was validated against the  
222 vessel segmented from the CT scan of the same phantom. The absolute  
223 surface-to-surface distance between the two models were computed after a  
224 rigid registration (Besl and McKay, 1992). For vascular navigation, one of  
225 the clinically relevant goals is to know the overall alignment of the vessels  
226 in space. To evaluate the spatial alignment, we used DICE metrics which  
227 compares the spatial overlap between the reconstructed and CT vessel af-  
228 ter CT-US registration was performed. False positive spatial region in the  
229 reconstructed US vessel is also an important metric and must be minimal  
230 to avoid the misrepresentation of the vessel. For many vascular procedures,  
231 the clinical objective is to avoid puncturing the vessels. In such cases, the  
232 boundary accuracy becomes important as well as the false positive regions.  
233 To evaluate the contours of the reconstructed vessel, we calculated the Haus-  
234 dorff distance (HD) metrics (Taha and Hanbury, 2015). Volumetric analysis  
235 was not performed as volume-based metrics are invariant of segmentation  
236 shape and boundary and thus can be misleading. As a visual validation, we  
237 demonstrate what US-based navigation may look like. A tracked, straight-  
238 tip guidewire(Piazza et al., 2020), augmented with a 5DOF EM sensor, was  
239 maneuvered to navigate the vessels in the phantom.

240 **Results**

241 The absolute distance between the US reconstructed vessel and the reg-  
 242 istered CT segmented vessel was computed and presented as a heatmap on  
 243 the vessel surface in Fig. 3c. The average distance between the surface of  
 244 the two models comes out to be  $1.7 \pm 1.12$  mm. A maximum error of 5.86 mm  
 245 between the two surface models was observed. The spatial overlap between  
 246 the registered US and CT models was evaluated using the Dice coefficient,  
 247 sensitivity and specificity measures using:

$$Dice = \frac{TP \text{ overlap between CT and US vessels}}{(num \text{ voxels CT vessel}) * (num \text{ voxels US vessel})} \quad (2)$$

$$Sensitivity = \frac{TP}{TP + FN} \quad (3)$$

$$Specificity = \frac{TN}{TN + FP} \quad (4)$$

248 where  $TP$ ,  $TN$ ,  $FP$  and  $FN$  represent the true positive, true negative,  
 249 false positive and false negative spatial overlap between the US and CT  
 250 segmented vessels respectively.

251 The spatial distance between the two model boundaries was evaluated  
 252 using the Hausdorff distance (HD). The geometric accuracy results are re-  
 253 ported in Table 1. Comparison showed that the US model had 12.93% false  
 254 negative and 6.60% false positive spatial overlap.

255 The x-ray imaging of our phantom, along with a guidewire, is represented  
 256 in Fig. 4a. In comparison, we can also achieve tool guidance using an US-  
 257 guided vascular navigation system. Fig. 4b shows how the US reconstructed  
 258 vessel looks like in 3D space. Virtual representation of a tracked guidewire  
 259 can be seen in context, as it navigates the phantom vessel.

## 260 **Discussion**

261 In this study, we present an vascular reconstruction-based surgical navi-  
262 gation system, which provides a safe and radiation-free method for guiding  
263 tools for X procedure. An EM-tracked ICE US probe was used to reconstruct  
264 the vascular path in a phantom, such that it can be visualized in a common  
265 coordinate system with a tracked guidewire for vessel navigation. The re-  
266 sults indicate that the average error in terms of HD is 1.7 mm, with a 3.16 mm  
267 confidence interval, which is a clinically acceptable value (Linte et al., 2010).  
268 During navigation, it is important to identify the vessel boundary and the  
269 regions outside the vessel lumen so as to not puncture or damage the vessel  
270 wall. Our results indicate that only 6.60% region lies outside the ground  
271 truth provided by the CT scan of the phantom. This over-segmentation is  
272 due to the leakages through the discontinuous wall boundary in some of the  
273 images when the ultrasound probe is clinging to the vessel wall. The ac-  
274 curacy of the navigation system can further be improved by improving the  
275 segmentation and tracking accuracy as discussed below.

276 The resulting error is a combination of many different errors in the system,  
277 such as EM tracking inaccuracies, propagation of calibration errors, US probe  
278 hardware constraints, registration errors, and relative motion of the phantom  
279 if any. One of the major limitations of our study is defined by the sensorizing  
280 the US probe and its calibration accuracy. This inaccuracy can be minimized  
281 by applying a manual offset correction for the imaging angle. The ICE probe  
282 used in this study has a small diameter of 3.3 mm which required rigidly  
283 fixing the sensor on the outer sheath of the probe, farther away from the  
284 origin of the image. The rigid and outer positioning of sensor lead to some

285 hardware constraints resulting in our inability to turn and guide the probe  
286 into the branches of the vessel. For a clinical system, the EM sensor must be  
287 integrated inside the US catheter to achieve accuracy in tracking, freedom  
288 in motion and patient safety from an active element. In the future, we  
289 plan to collaborate with the ICE probe manufacturers to acquire ICE probes  
290 embedded with EM sensors and designing a prototype of the US guidance  
291 system presented as a concept study in this paper.

292 The proposed US-based vascular navigation system can be implemented  
293 using many catheter-based US technology, such as radial IVUS probes that  
294 are regularly used during cardiac and endovascular interventions. Other than  
295 tracking, the accuracy of a clinical vessel reconstruction algorithm will also  
296 largely depend on the accuracy of lumen segmentation from in-vivo imag-  
297 ing. The appearance of a vessel in an intravascular or intracardiac US image  
298 varies significantly depending on the size and composition of the vessel, as  
299 well as the surrounding tissue and organs. The phantom images presented  
300 in this study replicate the US imaging of the infrarenal portion of IVC only.  
301 Even the echogenicity of the IVC changes as it passes through the abdomen.  
302 Thus a clinical system, implementing the proposed idea of US navigation,  
303 will require a robust deep learning-based segmentation pipe-line, which is  
304 capable of accurately identifying and segmenting all vascular structures as  
305 well as vessel branches and tributaries. Existing network architectures, such  
306 as U-Net, might be a suitable option for medical image segmentation. Since  
307 this is a pilot, proof of concept study for navigation with relatively restricted  
308 imaging data, we did not include any learning based approaches for segmen-  
309 tation and relied on conventional image processing techniques.

310 In future work we aim to improve this vascular reconstruction pipeline  
311 by replacing the image-processing based vessel segmentation algorithm with  
312 a deep learning-based segmentation technique trained on animal images ac-  
313 quired using the forward-looking, Foresight™ICE probe. The use of machine-  
314 learning for vascular segmentation and reconstruction has been previously  
315 performed using both surface US scans (Groves et al., 2020; Yang et al.,  
316 2013) and intravascular US (Yang et al., 2018). The integration of a machine-  
317 learning based segmentation will allow for accurate patient specific recon-  
318 structions to be obtained that account for differences in patients pathology.  
319 The segmentation algorithm can be trivially replaced within our vascular re-  
320 construction pipeline such that the different vessels required for navigation  
321 can be reconstructed using a robust segmentation algorithm capable of de-  
322 lineating various vascular morphologies and side vessel branches, allowing for  
323 safe navigation from the insertion site to the central venous system.

## 324 **Conclusions**

325 Transcatheter interventions provide a low-impact means of delivering  
326 therapy using miniaturized equipment and medical imaging technologies.  
327 Vascular navigation is a ubiquitous process as it is a prerequisite to reach the  
328 target organ or target site in another vessel. The current standard of care  
329 employs fluoroscopic techniques or the use of CT vascular mapping, both  
330 of which come at a cost of radiation exposure and wearing heavy, shielding  
331 aprons. Through this study, we aim to initiate a discussion on the merits  
332 of moving towards the use of ultrasound-based instead of radiation-based  
333 techniques for transcatheter and endovascular interventions. We present a

334 proof of concept study to use catheter-based US technology, equipped with  
335 tracking sensors, to create a vascular roadmap. Results indicate that the  
336 geometric accuracy is comparable to that observed in CT mapping. The  
337 concept demonstration (Fig. 4) shows side by side that an US-guided system  
338 can provide the same level of information and in three dimensions without  
339 the hazards of radiation and lead shielding.

#### 340 **Acknowledgements**

341 The authors would like to thank Dr. Dan Bainbridge (London Health  
342 Sciences Centre) and John Moore (Archetype Biomedical Inc.) for their  
343 valuable discussion and insight into the project. We acknowledge our sources  
344 of funding - Canadian Institutes of Health Research (CIHR) and Canadian  
345 Foundation for Innovation (CFI). The grants are held by Dr. Terry Peters.  
346 The authors would also like to thank Conavi Medical Inc. for providing the  
347 ultrasound imaging dataset.

348 **References**

- 349 Besl P, McKay ND. A method for registration of 3-d shapes. *IEEE Transactions on Pattern Analysis and Machine Intelligence*, 1992;14:239–256.
- 350
- 351 Chen ECS, Peters TM, Ma B. Guided ultrasound calibration: where, how,  
352 and how many calibration fiducials. *International Journal of Computer  
353 Assisted Radiology and Surgery*, 2016;11:889–898.
- 354 Christopoulos G, Makke L, Christakopoulos G, Kotsia A, Rangan BV,  
355 Roesle M, Haagen D, Kumbhani DJ, Chambers CE, Kapadia S, Mahmud  
356 E, Banerjee S, Brilakis ES. Optimizing Radiation Safety in the Cardiac  
357 Catheterization Laboratory. *Catheterization and Cardiovascular Interven-  
358 tions*, 2016;87:291–301.
- 359 Davenport MS, Cohan RH, Ellis JH. Contrast Media Controversies in 2015:  
360 Imaging Patients With Renal Impairment or Risk of Contrast Reaction.  
361 *American Journal of Roentgenology*, 2015;204:1174–1181.
- 362 Dixon RG, Khiatani V, Statler JD, Walser EM, Midia M, Miller DL, Bartal  
363 G, Collins JD, Gross KA, Stecker MS, Nikolic B. Society of Interventional  
364 Radiology: Occupational Back and Neck Pain and the Interventional Radi-  
365 ologist. *Journal of Vascular and Interventional Radiology*, 2017;28:195–199.
- 366 Fedorov A, Beichel R, Kalpathy-Cramer J, Finet J, Fillion-Robin JC, Pu-  
367 jol S, Bauer C, Jennings D, Fennessy F, Sonka M, Buatti J, Aylward S,  
368 Miller JV, Pieper S, Kikinis R. 3D Slicer as an image computing plat-  
369 form for the Quantitative Imaging Network. *Magnetic resonance imaging*,  
370 2012;30:1323–41.

- 371 Gao Y, Tannenbaum A, Kikinis R. Simultaneous multi-object segmenta-  
372 tion using local robust statistics and contour interaction. In: International  
373 MICCAI Workshop on Medical Computer Vision. Springer, 2010. pp. 195–  
374 203.
- 375 Goldstein JA, Balter S, Cowley M, Hodgson J, Klein LW. Occupational haz-  
376 ards of interventional cardiologists: Prevalence of orthopedic health prob-  
377 lems in contemporary practice. *Catheterization and Cardiovascular Inter-*  
378 *ventions*, 2004;63:407–411.
- 379 Groves LA, VanBerlo B, Veinberg N, Alboog A, Peters TM, Chen EC. Au-  
380 tomatic segmentation of the carotid artery and internal jugular vein from  
381 2d ultrasound images for 3d vascular reconstruction. *International journal*  
382 *of computer assisted radiology and surgery*, 2020.
- 383 Jacob S, Boveda S, Bar O, Brézin A, Maccia C, Laurier D, Bernier MO. In-  
384 terventional cardiologists and risk of radiation-induced cataract: Results  
385 of a French multicenter observational study. *International Journal of Car-*  
386 *diology*, 2013;167:1843–1847.
- 387 Jahangiri M, Hussain A, Akowuah E. Minimally invasive surgical aortic valve  
388 replacement. *Heart*, 2019;105:s10–s15.
- 389 Katsari K, Paraskevopoulou C, Barati M, Kostopoulou E, Griskevicius R,  
390 Blazquez N, Tekin HO, Illing RO. Lead exposure in clinical imaging—the  
391 elephant in the room. *European Journal of Radiology*, 2020;131:109210.
- 392 Limacher MC, Douglas PS, Germano G, Laskey WK, Lindsay BD, Mcketty  
393 MH, Moore ME, Park JK, Prigent FM, Walsh MN, Forrester JS, Faxon

394 DP, Fisher JD, Gibbons RJ, Halperin JL, Hutter AM, Kaul S, Skorton DJ,  
395 Weintraub WS, Winters WL, Wolk MJ. Radiation Safety in the Practice  
396 of Cardiology. Tech. rep., 1998.

397 Linte CA, Moore J, Peters TM. How accurate is accurate enough? A brief  
398 overview on accuracy considerations in image-guided cardiac interventions.  
399 In: 2010 Annual International Conference of the IEEE Engineering in  
400 Medicine and Biology. IEEE, 2010. pp. 2313–2316.

401 Little CD, Colchester RJ, Noimark S, Manmathan G, Finlay MC, Desjardins  
402 AE, Rakhit RD. Optically generated ultrasound for intracoronary imaging.  
403 Frontiers in Cardiovascular Medicine, 2020;7.

404 Murphy DJ, Aghayev A, Steigner ML. Vascular CT and MRI: a practical  
405 guide to imaging protocols. Insights into Imaging, 2018;9:215–236.

406 Murphy EA, Ross RA, Jones RG, Gandy SJ, Aristokleous N, Salsano M,  
407 Weir-McCall JR, Matthew S, Houston JG. Imaging in Vascular Access.  
408 Cardiovascular Engineering and Technology, 2017;8:255–272.

409 Nisar H, Moore J, Alves-Kotzev N, Hwang GYS, Peters TM, Chen ECS.  
410 Ultrasound calibration for unique 2.5D conical images. In: Fei B, Linte  
411 CA (Eds.), Medical Imaging 2019: Image-Guided Procedures, Robotic  
412 Interventions, and Modeling. SPIE, 2019. p. 78.

413 Nisar H, Moore J, Piazza R, Maneas E, Chen ECS, Peters TM. A sim-  
414 ple, realistic walled phantom for intravascular and intracardiac applica-  
415 tions. International Journal of Computer Assisted Radiology and Surgery,  
416 2020;15:1513–1523.

- 417 Piazza R, Nisar H, Moore J, Condino S, Ferrari M, Ferrari V, Peters T,  
418 Chen E. Towards electromagnetic tracking of J-tip guidewire: precision  
419 assessment of sensors during bending tests. In: Fei B, Linte CA (Eds.),  
420 Medical Imaging 2020: Image-Guided Procedures, Robotic Interventions,  
421 and Modeling. SPIE, 2020. p. 5.
- 422 Prendergast BD, Baumgartner H, Delgado V, Gérard O, Haude M, Him-  
423 melmann A, Iung B, Leafstedt M, Lennartz J, Maisano F, Marinelli EA,  
424 Modine T, Mueller M, Redwood SR, Rörick O, Sahyoun C, Saillant E,  
425 Søndergaard L, Thoenes M, Thomitzek K, Tschernich M, Vahanian A,  
426 Wendler O, Zemke EJ, Bax JJ. Transcatheter heart valve interventions:  
427 where are we? Where are we going? *European Heart Journal*, 2019;40:422–  
428 440.
- 429 Roguin A, Goldstein J, Bar O, Goldstein JA. Brain and Neck Tumors Among  
430 Physicians Performing Interventional Procedures. *The American Journal*  
431 *of Cardiology*, 2013;111:1368–1372.
- 432 Ross AM, Segal J, Borenstein D, Jenkins E, Cho S. Prevalence of Spinal  
433 Disc Disease Among Interventional Cardiologists. *The American Journal*  
434 *of Cardiology*, 1997;79:68–70.
- 435 Shammass N, Radaideh Q, Shammass WJ, Daher GE, Rachwan RJ, Radaideh  
436 Y. The role of precise imaging with intravascular ultrasound in coro-  
437 nary and peripheral interventions. *Vascular Health and Risk Management*,  
438 2019;Volume 15:283–290.
- 439 Stec S, Śledz J, Mazij M, Ras M, Ludwik B, Chrabaszcz M, Śledz A, Ba-

- 440 nasik M, Bzymek M, Mlynarczyk K, Deutsch K, Labus M, Śpikowski J,  
441 Szydłowski L. Feasibility of Implementation of a “Simplified, No-X-Ray,  
442 No-Lead Apron, Two-Catheter Approach” for Ablation of Supraventricu-  
443 lar Arrhythmias in Children and Adults. *Journal of Cardiovascular Elec-*  
444 *trophysiology*, 2014;25:866–874.
- 445 Taha AA, Hanbury A. Metrics for evaluating 3D medical image segmentation:  
446 analysis, selection, and tool. *BMC Medical Imaging*, 2015;15:29.
- 447 Theocharopoulos N, Damilakis J, Perisinakis K, Manios E, Vardas P, Gourt-  
448 soyiannis N. Occupational exposure in the electrophysiology laboratory:  
449 quantifying and minimizing radiation burden. *The British Journal of Ra-*  
450 *diology*, 2006;79:644–651.
- 451 Yang J, Tong L, Faraji M, Basu A. Ivus-net: an intravascular ultrasound  
452 segmentation network. In: *International Conference on Smart Multimedia*.  
453 Springer, 2018. pp. 367–377.
- 454 Yang X, Jin J, Xu M, Wu H, He W, Yuchi M, Ding M. Ultrasound common  
455 carotid artery segmentation based on active shape model. *Computational*  
456 *and mathematical methods in medicine*, 2013:345968.
- 457 Zhang G, Cheng L, Liang Z, Zhang J, Dong R, Hang F, Wang X,  
458 Wang Z, Zhao L, Wang Z, Wu Y. Zero-fluoroscopy transseptal puncture  
459 guided by right atrial electroanatomical mapping combined with intrac-  
460 ardiac echocardiography: A single-center experience. *Clinical Cardiology*,  
461 2020;43:1009–1016.

462 **Figure Captions**

463 **Figure 1:** Data acquisition setup - Ultrasound probe scans the vessel phan-  
464 tom present within the tracking space.

465 **Figure 2:** (a) Image data acquired using a framegrabber as a 2D projec-  
466 tion of the conical ultrasound. (b) Lumen segmentation (boundary)  
467 achieved using the initial seed (solid). (c) Conical reconstruction of the  
468 ultrasound image and the lumen segmentation.

469 **Figure 3:** Image a) depicts the skeleton of the vessel comprised of spatially  
470 calibrated segmentations, Image b) depicts the ultrasound (US) re-  
471 construction registered to the segmented CT scan of the phantom, and  
472 Image c) provides a visualization of the surface-to-surface distance anal-  
473 ysis between the US and CT models.

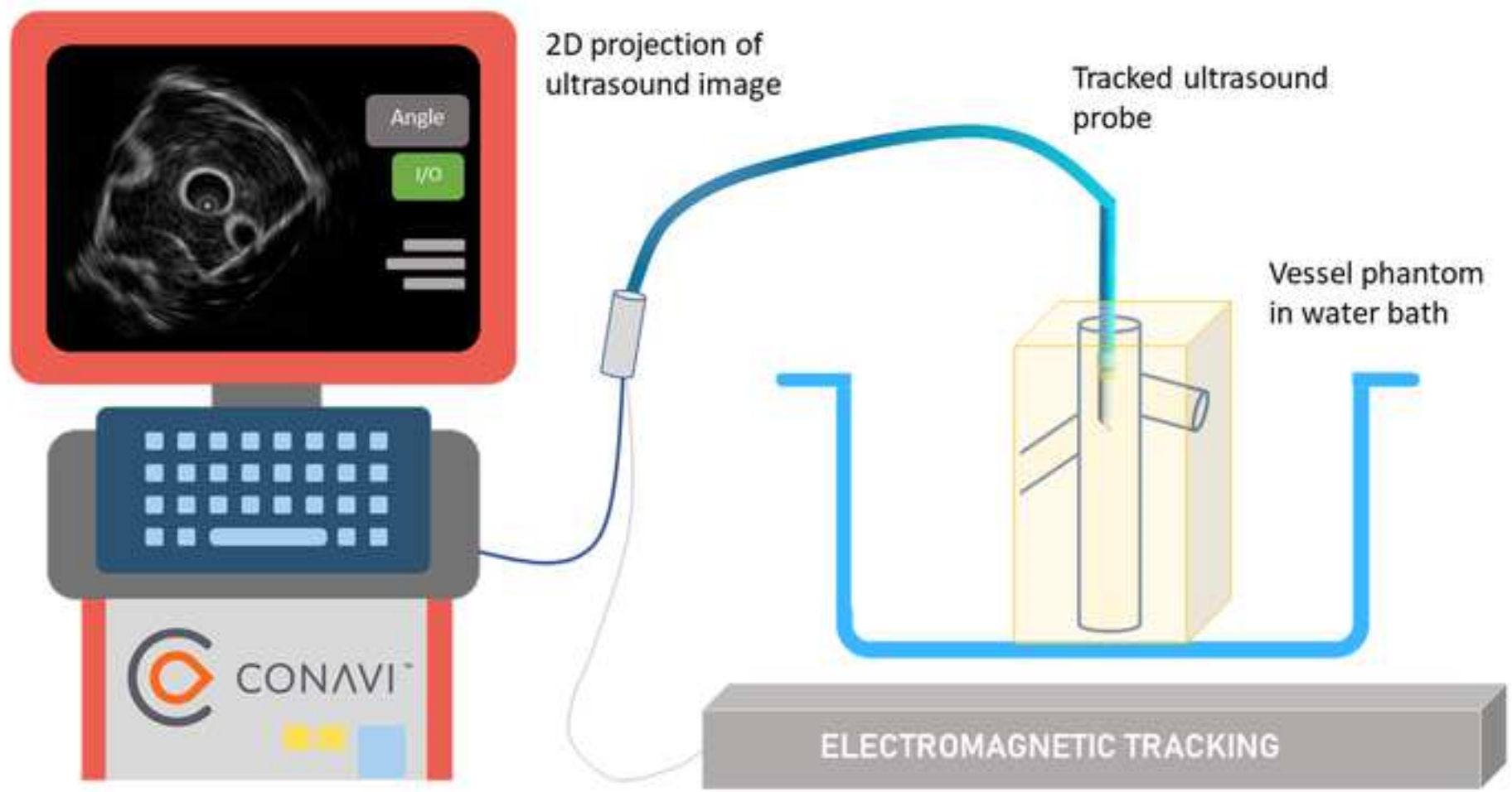
474 **Figure 4:** An example use case for navigating a tracked guidewire within the  
475 ultrasound reconstructed vessel (b) as compared to the fluoroscopic  
476 equivalent (a)

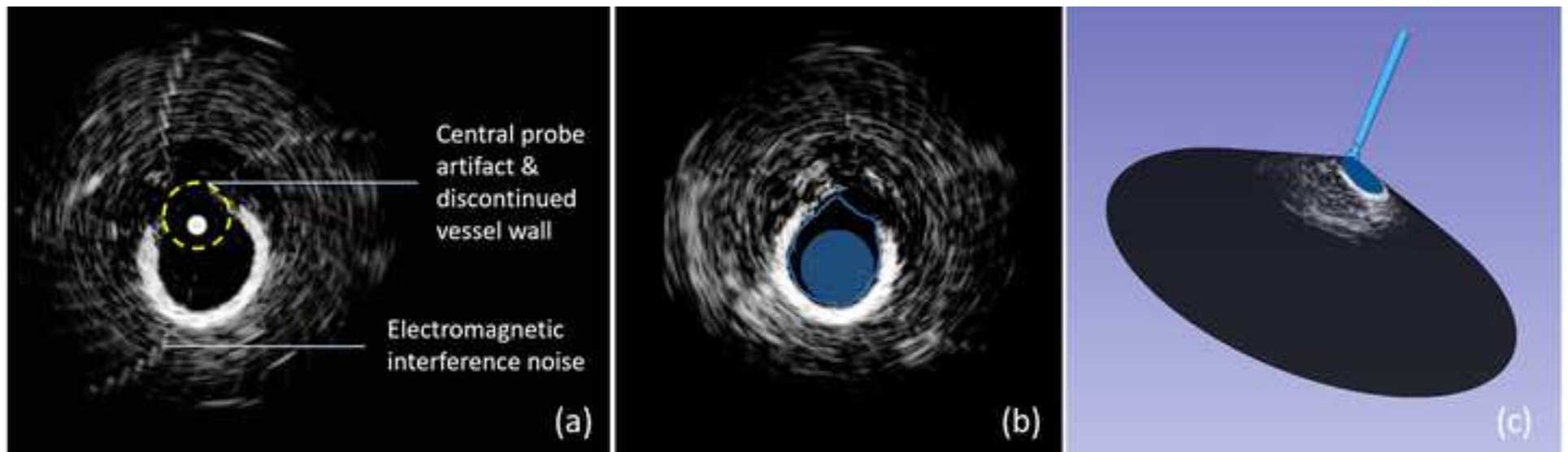
477 **Tables**

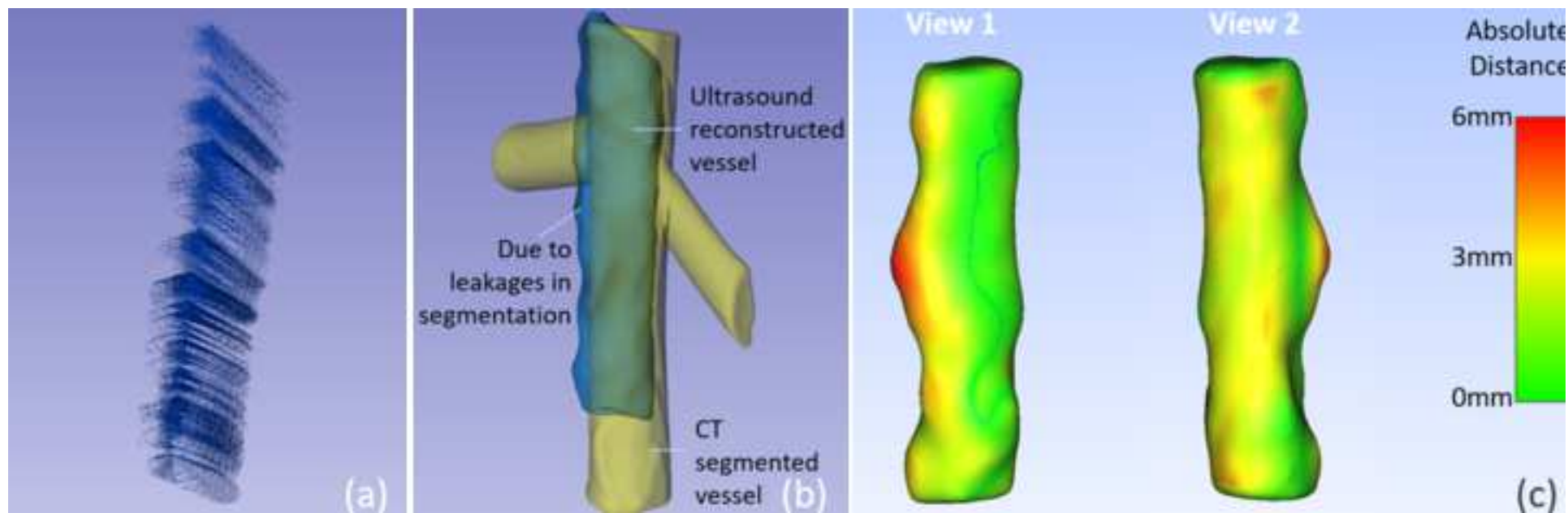
478 **Table 1:** Summary of the metrics use to quantify The spatial overlap and  
 479 boundary accuracy of the ultrasound reconstructed vessel compared to  
 480 the vessel segmented from the CT scan of the phantom.

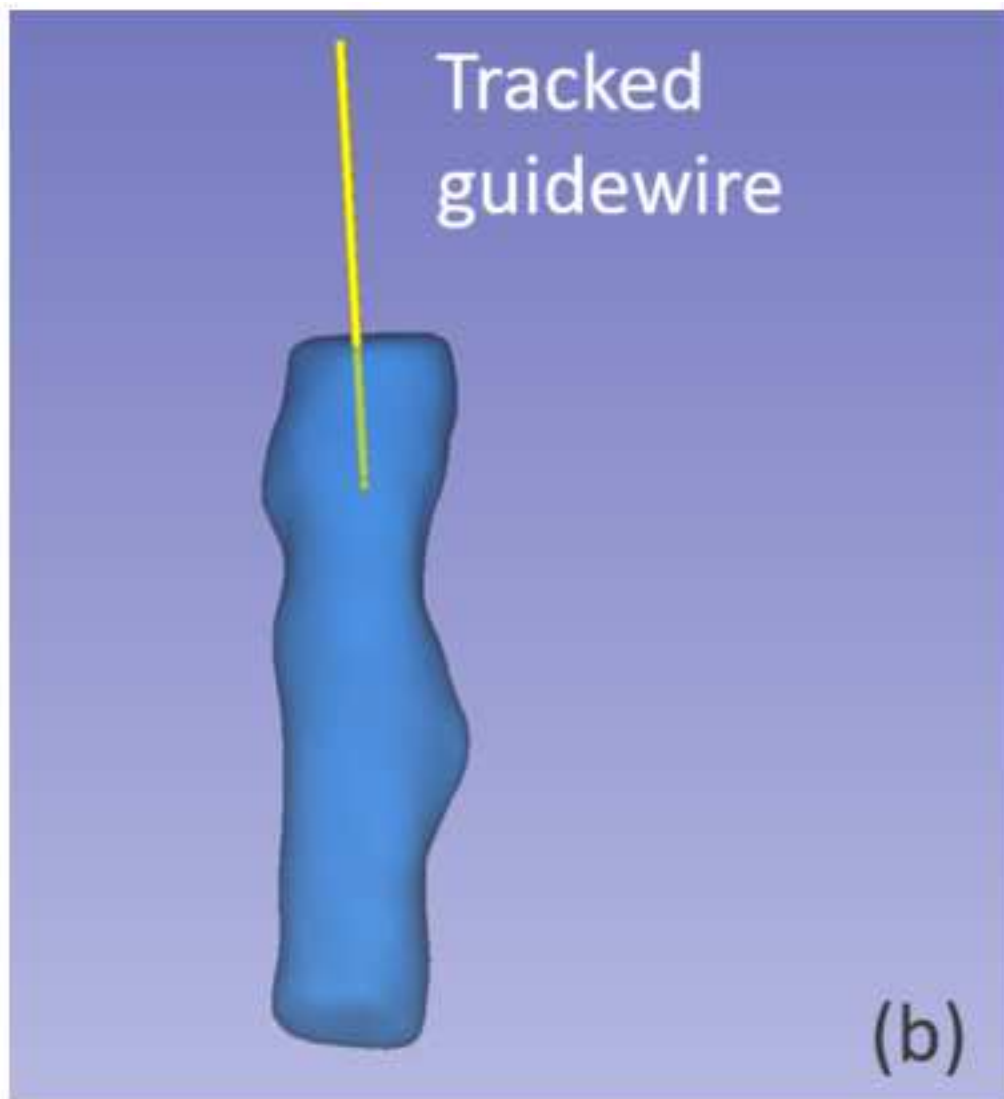
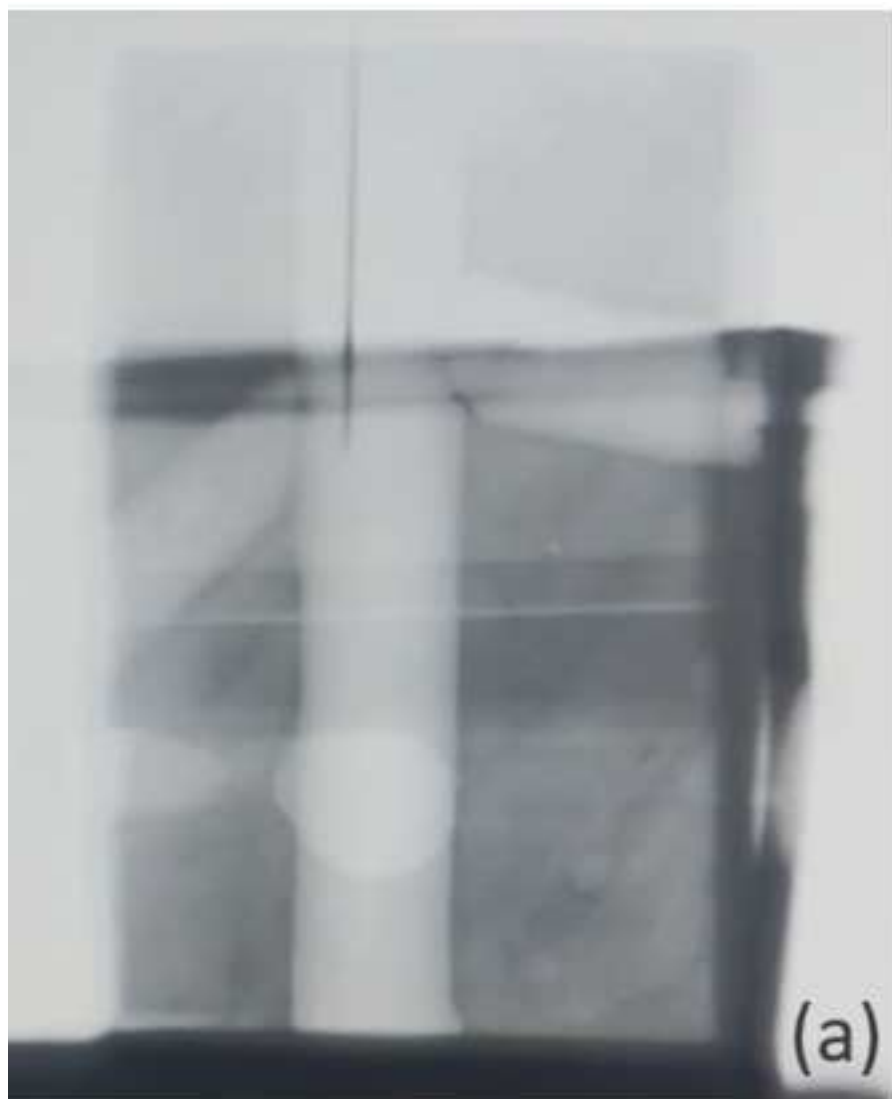
<b>Spatial Overlap</b>	<b>Value</b>	<b>Hausdorff Distance (mm)</b>	<b>Value</b>
DICE Coefficient	0.79	Maximum	5.86
Sensitivity	0.70	Average	1.63
Specificity	0.88	95 %	3.16

481











Click here to access/download  
**LaTeX Source Files**  
elsarticle.cls



Click here to access/download  
**LaTeX Source Files**  
UMB-elsarticle-harvbib.bst

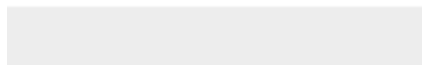
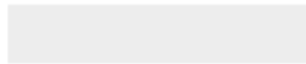




[Click here to access/download](#)

**LaTeX Source Files**

MAIN.tex

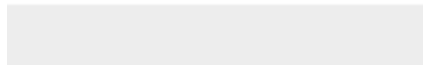




[Click here to access/download](#)

**LaTeX Source Files**

UMB2021BIB.bib





Click here to access/download

**LaTeX Source Files**

**UMB-elsarticle-template-harv.tex**

